

Mathematical Modelling of Nitric Oxide Release Caused by Exocytosis and Determination of a Stellate Neuron Activity Function in Rat Brain

A. Oleinick^{1,2}, C. Amatore², O. Klymenko¹, I. Svir^{1,2}

¹Kharkov National University of Radioelectronics
Mathematical and Computer Modelling Laboratory
14 Lenin Avenue, Kharkov, 61166, Ukraine
irina.svir@kture.kharkov.ua; irina.svir@ens.fr

²Ecole Normale Supérieure, Département de Chimie
UMR CNRS 8640 “PASTEUR”
24 rue Lhomond, 75231 Paris Cedex 05, France
christian.amatore@ens.fr

Received: 11.06.2007 **Revised:** 28.06.2007 **Published online:** 31.08.2007

Abstract. In this work we report the results of the mathematical modelling of NO^o-release by neurons considering a series of Gaussian bursts, together with its transport in the brain by diffusion. Our analysis relies on the NO^o-release from a neuron monitored *before*, *during* and *after* its patch-clamp stimulation as detected by an ultramicroelectrode introduced into a slice of living rat's brain. The parameters of the neuron activity function have been obtained by numerical fitting of experimental data with simulated theoretical results. Within our initial hypothesis about the Gaussian decomposition of NO^o-release that allowed drawing qualitative and quantitative conclusions about the considered neuron activity function. It is noted that since the activity function can be readily modified this signal processing may be adapted to the treatment of other and maybe more physiologically relevant hypotheses.

Keywords: brain slice, neuron activity function, nitric oxide release, Gaussian decomposition, conformal mapping, numerical fitting.

1 Introduction

In previous works [1, 2] we proposed two mathematical models and their numerical solution based on a conformal mapping approach for transport of nitric oxide emitted by a neuron during its stimulation within a slice of rat's brain. These works were aimed at obtaining the required overall direct component information about the processes under scrutiny by comparison between simulated theoretical results and experimental current data obtained through probing the NO^o concentration field with a microelectrode. As a result the direct component of the neuron NO^o-release activity function could be defined and quantitatively characterized.

Besides, the neuron activity function reconstructed numerically from experimental data allowed deducing the average nitric oxide concentration distribution in the vicinity of a neuron for the case when the microelectrode is absent in the considered system and thus does not interfere with the monitored concentration field. These results permitted the definition of the size of the brain area affected by the nitric oxide emitted by an active neuron, i.e. the area where the ensuing excess of nitric oxide may cause the dilatation of blood vessels in the brain. They also showed that the possible reaction between nitric oxide and oxygen was negligible over a large volume around the stimulated neuron.

On the other hand, it was noted, that current fluctuations occurring in the experimental data were significantly larger than those expected due to distortions induced by experimental equipment and other electrical noise sources. Here it has been supposed (as a *hypothesis*) that these current fluctuations reflect physiological issues leading to a discontinuous NO° release, viz., consisting of a series of single events corresponding to a sequence of bursts or to the sequential opening of NO° -releasing vesicles or vacuoles through the neuron surface. Here we use vacuolar or burst release indifferently since the physiological phenomena sustaining our hypothesis may still remain to characterize biologically. However, in this respect it should be noted that recent works [3, 4] have established that NO° can be released by a neuron into its environment and immediately cleared away by a re-uptake mechanism by the same neuron after the NO° neurotransmitter has performed its function. Under such circumstances, owing to the analogy between such process and that of dopamine release and uptake in the brain [5], one may readily predict that bell-shaped transient NO° bursts may be released by neurons. The overall phenomenology would then be similar to that of a vacuolar release [6] so that our present work would not be able to distinguish between the two of them.

In this work we thus propose to describe the neuron activity function as a linear combination of temporal spikes which are represented by Gaussian probability density functions. Each spike is assumed to represent NO° -release burst through the opening of a single vacuole or several ones. The neuron activity function is then represented by a superposition of sequential Gaussians. This model has allowed the reconstruction of current fluctuations in the experimental data on such basis. The parameters of the neuron activity function have been defined by numerical fitting of experimental data upon simulations of three independent experiments reported elsewhere [7, 8].

This work shows that it is experimentally reasonable to represent the NO° -release signals of neuron activity upon assuming a series of vacuolar releases, rather than a continuous release, though the correctness of this result should await physiological confirmation.

2 Theory

2.1 Mathematical model in the real and conformal spaces

Let us consider a living rat's brain slice containing the stimulated neuron and a microelectrode embedded inside of this slice (see Fig. 1). Experimental procedures for the slice preparation, neuron stimulation and current signal registration were described in details

in the previous publications from which the data used here have been extracted [7, 8]. In these experiments, the rat's brain slices were of thicknesses larger than $300 \mu\text{m}$, which is significantly larger than the size of the neuron-microelectrode system (few microns) positioned near the slice centre. Also, the stellate neurons investigated in these previous studies had spherical-type bodies. Therefore this system can be modelled by two spheres (spherical neuron and spherical ultramicroelectrode) which interact within an infinite space. Considering the intrinsic symmetry of the model only the half-plane shown in Fig. 2(a) needs to be considered. The neuron body and platinum microelectrode have radii r_1 (neuron) and r_2 (electrode), respectively. The distance between the neuron and electrode surfaces is g (see Fig. 2(a)). Nitric oxide (NO°) released by the neuron may spontaneously react with molecular oxygen (O_2) which is present within the rat's brain slice at an almost constant concentration [7,9]. However, as it was shown in work [1], this reaction can be ignored for the considered range of nitric oxide concentrations over the distances which matter in the investigated system. Furthermore NO° is able to diffuse at identical rates in aqueous and lipidic environments [10]. This ensures that the microscopic structure of the brain slice may be represented as a continuous medium for what concerns NO° diffusion, though the brain is heterogeneously structured.

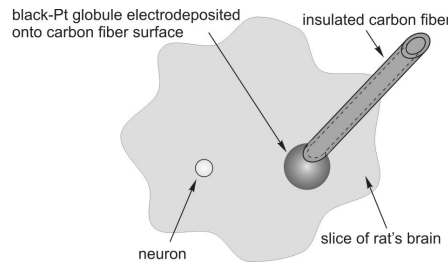


Fig. 1. Schematic view of the geometry of the system: neuron – ultramicroelectrode within a rat's brain slice.

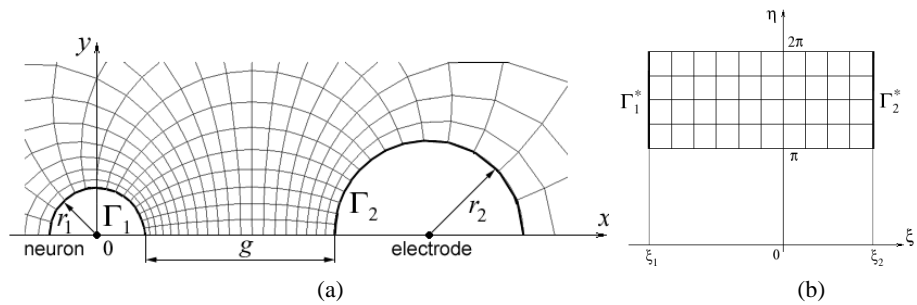


Fig. 2. Simulation area in real (a) and conformal coordinates (b).

Let us introduce the following dimensionless variables:

$$C = \frac{c}{c_0}; \quad X = \frac{x}{r_1}; \quad Y = \frac{y}{r_1}; \quad \tau = \frac{Dt}{r_1^2}, \tag{1}$$

where c is the nitric oxide concentration, c_0 is a reference nitric oxide concentration, t is the time, D is the nitric oxide diffusion coefficient.

The mathematical model in the dimensionless variables becomes:

$$\frac{\partial C}{\partial \tau} = \frac{\partial^2 C}{\partial X^2} + \frac{\partial^2 C}{\partial Y^2} + \frac{1}{Y} \frac{\partial C}{\partial Y}, \quad (2)$$

with the initial ($\tau = 0$):

$$\forall X, Y, \quad C = 0, \quad (3)$$

and boundary conditions ($\tau > 0$):

$$\begin{aligned} \forall X, Y \in \Gamma_1, \quad \frac{\partial C}{\partial \vec{N}} &= -\Phi(t) \quad (\text{neuron}), \\ Y = 0, X \in Sym, \quad \frac{\partial C}{\partial Y} &= 0 \quad (\text{symmetry axis}), \\ \forall X, Y \in \Gamma_2, \quad C &= 0 \quad (\text{electrode}), \\ X^2 + Y^2 \rightarrow \infty, \quad C &\rightarrow 0 \quad (\text{infinity}), \end{aligned} \quad (4)$$

where \vec{N} is a unit vector normal to the neuron surface; $\Phi(t)$ is the normalised neuron activity function, Sym is a part of the simulation area boundary corresponding to the symmetry axis, i.e. $Sym = \{X : X \in (-\infty, -1) \cup (1, 1 + G) \cup (P + R_2, +\infty)\}$, $P = 1 + G + R_2$.

In order to facilitate the numerical solution of the model (2)–(4) we apply a conformal mapping of the spatial coordinates proposed in [11]:

$$X = \frac{a e^{-\xi} - (a + b) \cos \eta + b e^{\xi}}{2(\cosh \xi - \cos \eta)}; \quad Y = \frac{(a - b) \sin \eta}{2(\cosh \xi - \cos \eta)}, \quad (5)$$

where a and b are the geometrical parameters of the investigated system:

$$a = \left[(1 + P^2 - R_2^2) - \sqrt{(1 + P^2 - R_2^2)^2 - 4P^2} \right] / 2P, \quad b = 1/a.$$

The coordinate transformation (5) maps the semi-infinite area shown in Fig. 2(a) (the upper half-plane minus two semicircles corresponding to the neuron and electrode) onto a rectangle (Fig. 2(b)). Therefore a uniform rectangular grid in the conformal coordinates (ξ, η) sketched in Fig. 2(b) corresponds to a non-uniform one in the real coordinates (x, y) in Fig. 2(a) [11].

The mathematical model in the transformed coordinates becomes [1]:

$$\frac{\partial C}{\partial \tau} = D^* \left[\frac{\partial^2 C}{\partial \xi^2} + \frac{\partial^2 C}{\partial \eta^2} \right] + \frac{1}{Y(\xi, \eta)} \left[\frac{\partial C}{\partial \xi} \frac{\partial \xi}{\partial Y} + \frac{\partial C}{\partial \eta} \frac{\partial \eta}{\partial Y} \right], \quad (6)$$

where

$$\begin{aligned} D^* &= \frac{4(\cosh \xi - \cos \eta)^2}{(a - b)^2}; \quad \frac{\partial \xi}{\partial Y} = -\frac{2 \sinh \xi \sin \eta}{a - b}; \\ \frac{\partial \eta}{\partial Y} &= -\frac{2(\cosh \xi \cos \eta - 1)}{a - b}, \end{aligned} \quad (7)$$

with the initial ($\tau = 0$)

$$\forall \xi, \eta, \quad C = 0, \quad (8)$$

and boundary conditions ($\tau > 0$):

$$\begin{aligned} \xi = \xi_1, \quad \pi \leq \eta \leq 2\pi, & \quad h_{\xi, \eta} \frac{\partial C}{\partial \xi} = -\Phi(\tau) \quad (\text{neuron}), \\ \xi_1 < \xi < \xi_2, \quad \eta = \pi, & \quad \frac{\partial C}{\partial \eta} = 0 \quad (\text{symmetry axis}), \\ \xi_1 < \xi < \xi_2 \quad (\xi \neq 0), \quad \eta = 2\pi, & \quad \frac{\partial C}{\partial \eta} = 0 \quad (\text{symmetry axis}), \\ \xi = \xi_2, \quad \pi \leq \eta \leq 2\pi, & \quad C = 0 \quad (\text{electrode}), \\ \xi = 0, \quad \eta = 2\pi, & \quad C = 0 \quad (\text{infinity}), \end{aligned} \quad (9)$$

where $h_{\xi, \eta} = 2(\cosh \xi - \cos \eta)/(b - a)$.

The transient current monitored by the microelectrode is defined as

$$i(t) = 2\pi F D c_0 r_2 \oint_{\Gamma_2} \frac{\partial C}{\partial \vec{N}} d\Gamma_2 = 2\pi F D c_0 r_2 \int_{\pi}^{2\pi} \frac{\sinh \xi \sin \eta}{\cosh \xi - \cos \eta} \frac{\partial C}{\partial \xi} \Big|_{\xi=\xi_2} d\xi, \quad (10)$$

where F is the Faraday constant; $d\Gamma_2$ is an element of the boundary Γ_2 (see Fig. 2(a)).

2.2 Identification of the neuron activity function

Let us consider a neuron activity function which describes one of “events” taking place on the neuron surface, i.e. vacuolar NO° -release (single or several vacuoles) and whose sequential superimposition gives rise to the overall current detected *in fine* by the microelectrode. We will call such an event a neuronal release spike. We assume that during each spike the change of nitric oxide flux produced at the neuron surface may be described by a single time-dependent Gaussian.

Note that the physiological consequences of this assumption for the characteristics obtained through this treatment (see Table 1) should be considered with care at this stage. The experimental physiological data that we rely on to demonstrate the applicability of our treatment have been already published [7, 8]. However, these were filtered to eliminate the high frequency noise since the aim of those studies was to extract the main direct component of the NO° release [1]. Therefore the fine structure, on which we base our experimental-theoretical analysis, may have been altered by the filtering process. This is why we may use hereafter a Gaussian decomposition since any sharp spike present in the original trace, if any, has been reduced into a Gaussian-like curve by the filtering process. Note that despite what has just been stated, this Gaussian assumption may be nevertheless realistic on physiological grounds. Indeed, it is supported by previous works which established that exocytosis of different active compounds (neurotransmitters [12],

oxidative burst [13]) can be described by curves resulting from the convolution of a normal distribution density function and an exponential one. In this work we use only a normal distribution density function (Gaussian), which amounts to consider that the exponent is close to zero. This is for simplicity but also takes into account the existence of filtering of the data to be treated.

Assigning a single Gaussian to each release spike in the current and summing them we obtain the overall activity function of the neuron as:

$$D \frac{\partial c}{\partial \bar{n}} = -\phi(t) = -\sum_{i=1}^m \phi_i(t) = -\sum_{i=1}^m \varphi_i \exp \left[-\frac{(t-t_i)^2}{\sigma_i^2} \right], \quad (11)$$

where $\phi(t)$ is the overall neuron activity function; $\phi_i(t)$ is a function describing i th spike (i.e., the individual release function); φ_i is the amplitude of i th spike; σ_i is the parameter responsible for the width of the i th spike and is related to the peak width at its half height, Δ_i (as $\Delta_i = 2\sigma_i\sqrt{\ln 2}$); t_i is the time position of the i th spike maximum relative to the initial time; and m is the number of spikes required to describe the recorded response.

The neuron activity function in the dimensionless variables then becomes:

$$\frac{\partial C}{\partial \bar{N}} = -\Phi(\tau) = -\sum_{i=1}^m \Phi_i(\tau) = -\sum_{i=1}^m \varphi_i^* \exp \left[-\frac{(\tau-\tau_i)^2}{\sigma_i^{*2}} \right], \quad (12)$$

where $\varphi_i^* = r_1\varphi_i/Dc_0$ and $\sigma_i^* = D\sigma_i/r_1^2$ are the dimensionless amplitude and width of i th spike, respectively.

2.3 Nitric oxide released quantity: definition

Using the representation of the nitric oxide flux at the neuron surface in the form of a linear combination of Gaussians one can calculate the quantity of nitric oxide matter (and hence the number of molecules) emitted by the neuron either during any segment of the whole observation period or during one spike of neuronal activity which corresponds to the vacuolar release (single or several) at the neuron surface (see (11)). As indicated above, the latter one “event” may be described by a single Gaussian so that the quantity of nitric oxide emitted by the neuron during one spike of activity can be obtained by integrating the flux of nitric oxide through the neuron surface during the neuronal activity when the neuron activity function consists of a single Gaussian:

$$\begin{aligned} M_i = N_A N_i &= N_A \int_{-\infty}^{\infty} \int_S D \frac{\partial c}{\partial \bar{n}} dS dt \\ &= N_A 4\pi r_1^2 \varphi_i \int_{-\infty}^{\infty} \exp \left[-\frac{(t-t_i)^2}{\sigma_i^2} \right] dt = N_A 4\pi^{3/2} r_1^2 \varphi_i \sigma_i, \end{aligned} \quad (13)$$

where M_i , N_i are the number of molecules and quantity (in moles) of nitric oxide emitted by the neuron during i th spike of activity; N_A is the Avogadro number. Hereafter we

will consider only M_i values, viz., we will count the released quantities in molecules rather than in moles to account for their extremely minute values (a few tens of millions of molecules; see Table 1).

Table 1. Average and expected values of characteristics of stellate neuron activities: *before, during and after stimulation**

Neuron activity parameters	Experimental series	<i>Before</i> neuron stimulation	<i>During</i> neuron stimulation	<i>After</i> neuron stimulation
\overline{M}_i , million molecules	I	27 ± 17	100 ± 70	12 ± 9
	II	27 ± 24	380 ± 226	37 ± 46
	III	41 ± 36	134 ± 102	24 ± 20
$\overline{\Delta}$, s	I	8.0 ± 2.4	10.1 ± 3.5	5.6 ± 1.9
	II	4.9 ± 2.5	13.2 ± 4.2	4.9 ± 2.9
	III	4.0 ± 1.8	3.4 ± 1.3	2.2 ± 0.9
$(\overline{t_i - t_{i-1}})$, s	I	12.2 ± 4.1	10.4 ± 3.6	6.7 ± 3.5
	II	4.6 ± 3.1	11.4 ± 3.8	7.1 ± 5.1
	III	3.9 ± 1.9	2.82 ± 2.1	2.1 ± 1.1
Ψ_{mean}^j , million molecules/s	I	2.2 ± 0.2	9.7 ± 0.2	1.7 ± 0.2
	II	5.4 ± 0.5	33.1 ± 0.7	5.1 ± 0.5
	III	10.0 ± 1.0	50.0 ± 1.0	9.2 ± 0.9

*Notation \overline{x} stands for the expected value and x_{mean} for the mean value of the variable. \overline{M}_i is the expected value of number of molecules emitted by the neuron over each phase duration, $\overline{\Delta} = 2\sigma\sqrt{\ln 2}$ is the expected value of peak width at its half height, $(\overline{t_i - t_{i-1}})$ is the expected value of peak-to-peak separation between two adjacent Gaussian spikes, Ψ_{mean}^j is the mean value of the nitric oxide flux at the neuron surface.

3 Results of simulations and their discussion

Fig. 3(a) illustrates one typical measurement of stimulated NO° -release (black solid line) for an experiment involving the following parameters: $r_1 = 5 \mu\text{m}$, $g = 10 \mu\text{m}$ and $r_2 = 10 \mu\text{m}$. The value of the diffusion coefficient used in this study was taken $D = 10^{-5} \text{cm}^2 \text{s}^{-1}$ being the generally accepted average diffusion coefficient for the nitric oxide through lipidic phases and aqueous media [10]. For comparison, the superimposed light solid thicker line illustrates the results of numerical simulations according to the neuron activity function defined in (11). The horizontal line segments in Fig. 3 show the duration of the neuron patch-clamp stimulation. As one can see from Fig. 3(a) the current fluctuations can be reconstructed very accurately for the considered experimental nitric oxide flux using a combination of Gaussians (11). The series of individual spike functions, $\phi_i(t)$, represented by Gaussians whose parameters were extracted by fitting experimental (Fig. 3(a)) and theoretical data are shown in Fig. 3(b). Fig. 3(c) presents the overall reconstructed neuron activity function, ϕ . From Fig. 3(c) one can see that the neuron activity function has practically the same shape as the current registered at the microelectrode or its simulation in Fig. 3(a). This observation confirms the conclusion

made in [1], i.e. that diffusion filtering of the initial nitric oxide flux emitted at the neuron surface is negligible and causes only an overall delay of tenths of a millisecond in the electrode response. The latter filtering was duly simulated in the theoretical response shown in Fig. 3(a), though its effect is not visible at all on the time scale (hundreds of seconds).

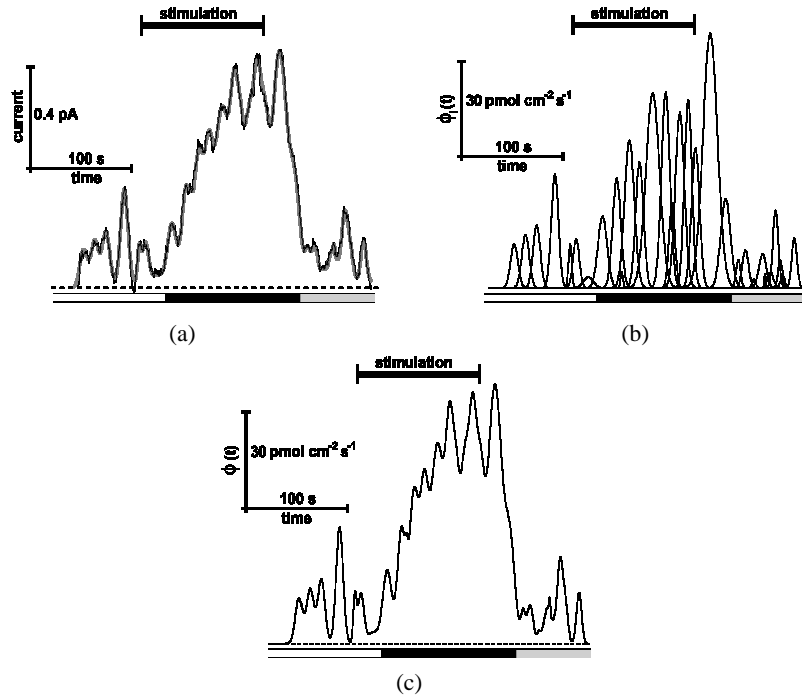


Fig. 3. Representation of a typical stellate neuron activity function as deduced from in situ measurement by a black-platinum ultramicroelectrode: (a) experimental (black curve) and best-fit currents (light curve); (b) Gaussian decomposition; (c) reconstructed signal considering the Gaussian decomposition shown in (b). Note that the reconstructed trace in (a) derives from the function in (c) convoluted by diffusion to the ultramicroelectrode. The bar under each plot indicates the different phases of neuronal activity: white color – before the start of stimulated activity, black color – during the effective activity, grey color – after the effective activity. The experimental patch-clamp stimulation duration is shown above each curve by the linear segment.

The average behavior of the neuron *before*, *during* and *after* the stimulation can be characterized by average values of the neuron activity function parameters within each of these stages, i.e. by the average values of M_i , Δ , $(t_i - t_{i-1})$ and Ψ^j . The parameter $(t_i - t_{i-1})$ represents the average time delay between two consecutive spikes so that it reflects the frequency of spikes. $\Psi_{mean}^j = \sum M_i / \Delta t_j^{phase}$ is the average flux (in molecules per second) emitted by the neuron during each phase indicated by the bar

coding in Figs. 3(a)–(c), where the summation is over all spikes in j th phase and Δt_j^{phase} is the recorded duration of this phase.

The averaged values of these parameters are given in the Table 1 for the experimental data given in Fig. 3(a) together with two other experimental signals, which have already been reported elsewhere (see Fig. 4 in [1]). The obtained data show that during the stimulation phase (i) the nitric oxide bursts occur more often, (ii) spikes have larger amplitude and (iii) are more protracted (the Δ value, and therefore the width of the spike, is increased), than before stimulation. When the stimulation ends up, within the precision of its determination, the parameters of the spikes practically revert to their initial values before the stimulation. Each value in Table 1 is given with the respective standard deviation calculated using unbiased estimations. The standard deviation for the averaged flux of the nitric oxide was evaluated as average deviation between the experimental and best-fit theoretical signals within a given phase.

4 Conclusion

In this work we examined the feasibility and precision of a theoretical approach to the modelling of nitric oxide mass release within brain tissues, based upon considering a neuron activity function consisting of a succession of “single events”, e.g., of a series of bursts occurring at the neuron surface. The proposed model has allowed adequate reconstruction of the experimentally significant current fluctuations observed in the experimental data. Within the Gaussian-type description used here, the parameters of the neuron activity function obtained by fitting of experimental data by simulated theoretical results allow the extraction of important information about NO° -release by the neuron *before*, *during* and *after* its patch-clamp stimulation. Additionally, it allows the evaluation of the nitric oxide quantity emitted by the neuron during each individual burst which appears meaningful physiologically compared to other examples on vacuolar or vesicular releases. This representation of the neuron activity function as a superposition of Gaussians can be easily adapted to a more sophisticated description and treatment involving more sound physiological interpretations.

Acknowledgments

The authors thank NATO for the grant CLG.981957 and the Ukrainian Ministry of Education and Science for supporting this project between two research groups of Prof. Irina Svir (Ukraine) and Prof. Christian Amatore (France). Dr. Oleinick thanks INTAS for post-doc by YSF (06-100019-6451). Prof. Svir expresses her many thanks to CNRS for her Director of Research position at ENS (Paris, France).

References

1. A. Oleinick, C. Amatore, M. Guille, S. Arbault, O. Klymenko, I. Svir, Modelling release of nitric oxide in a slice of rat’s brain: describing stimulated functional hyperemia with diffusion-

- reaction equations, *Math. Med. Biol.*, **23**, pp. 27–44, 2006.
2. A. Oleinick, C. Amatore, I. Svir, Mathematical models and numerical simulation of diffusion-reaction problems of brain-chemistry, *Radioelek. Inform.*, **3**, pp. 18–22, 2005.
 3. J. Sullivan, NO going back, *Nat. Neurosci.*, **6**, pp. 905–906, 2003.
 4. K. D. Micheva, J. Buchanan, R. W. Holz, S. J. Smith, Retrograde regulation of synaptic vesicle endocytosis and recycling, *Nat. Neurosci.*, **6**, pp. 925–932, 2003.
 5. R. M. Wightman, C. Amatore, R. C. Engstrom, P. D. Half, E. W. Kristensen, W. C. Kuhr, L. J. May, Real-time characterization of dopamine overflow and uptake in the rat striatum, *Neurosci.*, **25**, pp. 513–523, 1988.
 6. C. Amatore, S. Arbault, Y. Chen, C. Crozatier, I. Tapsoba, Electrochemical detection in a microfluidic device of oxidative stress generated by macrophage cells, *Lab Chip*, **7**, pp. 233–238, 2007.
 7. C. Amatore, S. Arbault, Y. Bouret, B. Cauli, M. Guille, A. Rancillac, J. Rossier, Detection of Nitric Oxide Release During Neuronal Activity with Platinized Carbon Fiber Microelectrodes, *ChemPhysChem.*, **7**, pp. 181–187, 2006.
 8. A. Rancillac, M. Guille, X.-K. Tong, H. Geoffroy, E. Hamel, C. Amatore, S. Arbault, J. Rossier, B. Cauli, Glutamatergic Control of Microvascular Tone by Distinct GABA Neurons in the Cerebellum, *J. Neuroscience*, **26**, pp. 6997–7006, 2006.
 9. V. L. Pogrebnaya, A. P. Usov, A. V. Nesterenko, P. I. Bez'yazychnyi, Oxidation of nitric-oxide by oxygen in liquid-phase, *J. Appl. Chem. USSR*, **48**, pp. 954–958, 1975.
 10. A. Denicola, J. M. Souza, R. Radi, E. Lissi, Nitric Oxide Diffusion in Membranes Determined by Fluorescence Quenching, *Arch. Biochem. Biophys.*, **328**, pp. 208–212, 1996.
 11. C. Amatore, A. Oleinick, I. Svir, Simulation of the Double Hemicylinder Generator-Collector Assembly through Conformal Mapping Technique, *J. Electroanal. Chem.*, **553**, pp. 49–61, 2003.
 12. C. Amatore, Y. Bouret, L. Midrier, Time Resolved Dynamics of the Vesicle Membrane During Individual Exocytotic Secretion Events as Extracted from Amperometric Monitoring of Adrenaline Exocytosis by Chromaffin Cells, *Chem. Eur. J.*, **5**, pp. 2151–2162, 1999.
 13. C. Amatore, S. Arbault, C. Bouton, K. Coffi, J.-C. Drapier, H. Ghandour, Y. Tong, Monitoring the Release of Reactive Oxygen and Nitrogen Species by a Single Macrophage in Real-Time with a Microelectrode, *ChemBioChem.*, **7**, pp. 653–661, 2006.